Atmos. Chem. Phys. Discuss., doi:10.5194/acp-2017-470, 2017
Manuscript under review for journal Atmos. Chem. Phys.
Discussion started: 29 May 2017

Changing transport processes in the stratosphere by radiative heating of sulfate aerosols

Ulrike Niemeier[1] and Hauke Schmidt[1]
[1]Max Planck Institute for Meteorology, Bundesstr. 53, 20146 Hamburg, Germany
Correspondence to: U. Niemeier (ulrike.niemeier@mpimet.mpg.de)

Abstract. The injection of sulfur dioxide (SO_2) into the stratosphere to form an artificial stratospheric aerosol layer is discussed as an option for solar radiation management. Sulfate aerosol scatters solar radiation and absorbs infrared radiation, which warms the stratospheric sulfur layer. Simulations with the general circulation model ECHAM5-HAM, including aerosol microphysics, show consequences of this warming, including changes of the quasi biennial oscillation (QBO) in the tropics. The QBO slows down after an injection of 4 $\mathrm{Tg(S)yr^{-1}}$ and completely shuts down after an injection of 8 $\mathrm{Tg(S)yr^{-1}}$. Transport of species in the tropics and sub-tropics depends on the phase of the QBO. Consequently, the heated aerosol layer not only impacts the oscillation of the QBO but also the meridional transport of the sulfate aerosols. The stronger the injection, the stronger the heating and the simulated impact on the QBO and equatorial wind systems. With increasing injection rate the velocity of the equatorial jet streams increases, and less sulfate is transported out of the tropics. This reduces the global distribution of sulfate and decreases the radiative forcing efficiency of the aerosol layer by 10% to 14% compared to simulations with low vertical resolution and without generated QBO. Increasing the height of the injection increases the radiative forcing only for injection rates below 10 $\mathrm{Tg(S)yr^{-1}}$ (8 - 10%), a much smaller value than the 50% calculated previously. Stronger injection rates at higher levels even result in smaller forcing than the injections at lower levels.

1 Introduction

A large natural source of sulfur in the stratosphere is volcanic sulfur dioxide (SO_2). It is known from observations that stratospheric sulfate from a volcanic eruption impacts the climate and influences also stratospheric dynamics. For example, winter warmings observed in regions of the northern hemisphere after the eruptions of Mt Pinatubo and Mt Krakatoa are caused by dynamical changes

Atmos. Chem. Phys. Discuss., doi:10.5194/acp-2017-470, 2017
Manuscript under review for journal Atmos. Chem. Phys.
Discussion started: 29 May 2017

Atmospheric Chemistry and Physics
Open Access
Discussions

in the stratosphere (Robock (2000), Shindell et al. (2004)). Changes to the quasi biennial circulation (QBO) (Labitzke, 1994) and the polar vortex (e.g. Bittner et al. (2016)) were also observed. Stratospheric sulfur acts as a reflector and also as an absorber. The sulfate aerosol scatters solar radiation (short wave, SW) and absorbs in the nearby infrared and infrared (long wave, LW) radiation bands. The scattering causes a cooling of the surface and the absorption a heating of the stratospheric aerosol layer.

The cooling of the earth's surface observed after the emission of volcanic aerosols is considered a natural example for potential effects of the proposed climate engineering (CE) technique of injecting sulfur into the stratosphere (Budyko (1977), Crutzen (2006)). Such surface cooling is intended but numerical CE studies show that the artificial climate under CE would not be the same as a natural one under the same forcing conditions (Schmidt et al., 2012) because CE changes the hydrological cycle (Tilmes et al. (2013), Kravitz et al. (2013)) due to different effects in the top of the atmosphere (TOA) and surface radiative imbalance (Niemeier et al., 2013). An impact of the warming in the stratosphere on stratospheric dynamics was discussed by Aquila et al. (2014) who simulate changes to the quasi-biennial circulation caused by sulfur injection. After the injection of $1.25\,\mathrm{Tg(S)yr^{-1}}$ the westerly phase of the QBO starts to be prolonged in the lower stratosphere and the oscillation vanished with the injection of $2.5\,\mathrm{Tg(S)yr^{-1}}$. These changes in the QBO are triggered by two processes: changes in the thermal wind balance and increased residual vertical wind velocity. The phase of the QBO influences transport processes in the tropics (Plumb (1996), Haynes and Shuckburgh (2000)) and extratropics (Punge et al., 2009). The impact of sulfur injections on the QBO should, therefore, also impact transport processes in the stratosphere in addition to the acceleration of the Brewer Dobson Circulation (BDC) described in Aquila et al. (2014). The main intention of our study is to determine how changes of the transport of sulfate aerosol in the stratosphere are dependent on the state of the QBO and the jets in the tropical stratosphere. This work was performed with the General Circulation Model ECHAM5 (Roeckner et al., 2003) coupled to an aerosol microphysics model (HAM) (Stier et al., 2005). We raised the question if ECHAM5-HAM simulates similar impacts on the QBO as described in Aquila et al. (2014) and which consequences this has for dynamical processes in the stratosphere, the global distribution of sulfate aerosol and the cooling efficiency of the artificial aerosol layer.

Niemeier and Timmreck (2015) determined the efficiency of sulfur injections depending on injection rate and injection area. They define a forcing efficiency: the relation of top of the atmosphere (TOA) radiative forcing of sulfate to the injection rate. They also discussed the impact of the subtropical transport barrier on the efficiency. A stronger barrier results in lower efficiency. Aquila et al. (2014) show an intensification of the equatorial jet caused by the impact of sulfur injections. A stronger jet is related to a stronger transport barrier (Bowman, 1996). Therefore, we discuss the efficiency of the sulfur injection and compare to earlier results (Niemeier and Timmreck, 2015). In this study, the aerosols are mostly injected in the tropics as this shows the strongest forcing efficiency in

Atmos. Chem. Phys. Discuss., doi:10.5194/acp-2017-470, 2017
Manuscript under review for journal Atmos. Chem. Phys.
Discussion started: 29 May 2017

our model (Niemeier and Timmreck, 2015). Injections over a wider latitude band, also outside the tropics, reduces the aerosol load in the tropics and, thus, the impact on the QBO.

This paper is structured as follows: We give a brief general overview of stratospheric dynamics and the QBO (Section 2) and summarize the explanation given by Aquila et al. (2014) of how the heated sulfate layer impacts the QBO. The model setup and the simulations performed in this work are described in Section 3. The results of these simulations are described in three parts. The implication of sulfur injections on: stratospheric dynamics in Section 4; the transport of sulfate in Section 5) and the radiative forcing and the efficiency of the injection in Section 6.

2 Stratospheric dynamics and transport — a short overview

2.1 Circulation in the stratosphere

Long-living species such as ozone are transported in a global-scale stratospheric transport regime with rising air in the tropics, the 'tropical pipe' (Plumb, 1996), and descending air at the poles. The stratospheric meridional residual circulation is known as Brewer Dobson Circulation (BDC). The tropical pipe is related to an area of very low horizontal mixing and high zonal wind speed, the tropical jets of the QBO. Breaking Rossby and gravity waves drive the BDC and cause a strong seasonal dependency with strong transport towards the winter hemisphere of midlatitudes. Additionally, breaking planetary waves cause rapid isentropical, quasi-horizontal mixing in the lower stratosphere. This 'surf zone' reaches from the subtropics to high latitudes (Holton et al., 1995) and combines fast meridional transport with the slow BDC (Butchart et al., 2006). This quasi-horizontal mixing is the main transport branch for the sulfate aerosol.

Sharp gradients of potential vorticity at the edges of the surf zone act as a transport barrier: the polar vortex at high latitudes inhibits transport to the poles in winter months and the equatorial jets of the QBO form, at this edges, the subtropical transport barrier. This subtropical barrier results in the formation of a reservoir for chemical species in the lower tropical stratosphere (Trepte and Hitchman, 1992). The barrier is strongest in heights between 21 km to 28 km (50 to 15 hPa). The strength of the transport barrier is related on the wind speed of the jet because the barrier can be interpreted as a result of the lack of waves with fast phase speeds compared to the speed of the jet (Bowman, 1996). These barriers can be seen as 'eddy-transport-barriers'. They do not act as barriers to the zonally averaged BDC (Haynes and Shuckburgh, 2000).

A schematic diagram of the transport pattern in the stratosphere is e.g. given in Haynes and Shuckburgh (2000). Butchart (2014) provides an overview of the stratospheric dynamic processes described above, as well as related references.

Atmos. Chem. Phys. Discuss., doi:10.5194/acp-2017-470, 2017
Manuscript under review for journal Atmos. Chem. Phys.
Discussion started: 29 May 2017

2.2 QBO and stratospheric dynamical processes

The QBO is formed by alternating westerly and easterly winds with an average period of about 29 month at the equator. The phases of the wind propagate from the upper stratosphere (about 5 hPa) downward into the tropopause region.

Observations and previous studies show that transport processes in the stratosphere depend on the phase of the QBO (Plumb and Bell (1982)). Equatorward motion in the westerly jet and poleward motion in the easterly jet are both a consequence of the Coriolis force (β effect). This extends the dynamical structure in the tropics into the subtropics, the circulation is named secondary meridional Circulation (SMC). Within the tropical pipe the air is rising but the SMC intensifies the vertical velocity in easterly QBO shear and lessens it in westerly QBO shear.

The described diabatic circulation is accompanied by isentropic mixing. The isentropic transport in the different QBO phases has been analyzed in detail by O'Sullivan and Chen (1996), Shuckburgh et al. (2001), and Punge et al. (2009). Shuckburgh et al. (2001) and Punge et al. (2009) describe for QBO westerlies a narrow region at the Equator where mixing is inhibited. The surf zone reaches far into the tropics in the winter hemisphere, going from 5° to the mid-latitudes, and a second surf zone develops between 5° and 15° in the summer hemisphere because the QBO westerlies allow the penetration of waves through the tropics into the summer hemisphere. This causes mixing from the tropics into the sub-tropics The waves get damped where winds become easterly, causing enhanced mixing in this area (about 20° N and S) (Punge et al., 2009). QBO winds have an impact on extratropical wave propagation as westerly winds allow in general the propagation of these waves, different to easterly winds.

2.3 QBO and radiative heating of sulfate aerosol

Aquila et al. (2014) simulate changes of the oscillation of the QBO caused by injection of sulfur into the stratosphere. Injecting 2.5 $\mathrm{Tg(S)yr^{-1}}$, the oscillation slows down and phases with westerly wind in the lower stratosphere are prolonged, Injecting at higher altitude causes the oscillation to break down and a constant westerly wind develops in the lower stratosphere. They show an acceleration of the BDC in the tropics and mid-latitudes, but only a small impact on the high-latitude branches of the BDC.

Stratospheric sulfate absorbs infra-red radiation which warms the lower stratosphere. This radiative heating has two consequences: a disturbed thermal wind balance and an increased residual vertical velocity ω^* (Niemeier et al., 2011). Temperature and vertical wind shear are approximately in thermal wind balance (Andrews et al. (1987) and Baldwin et al. (2001), Eq. 1b for details). Thus, the consequence of the heated aerosol layer is a vertical wind shear causing an additional westerly component of the zonal wind above the heated aerosol layer resulting in the prolonged phases of westerlies in the lower stratosphere. The increase of ω^* extends to much higher vertical levels than just the heating of the aerosols (Aquila et al., 2014). This stronger ω^* causes a westerly momentum forcing from the vertical advection of the zonal wind component $(-\omega^* u_z)$ which over-compensates downward easterly momentum transfer from gravity wave dissipation (Aquila et al., 2014). Once this strengthening of the upward advection overwhelms the wave mean-flow interaction in the shear layer, which causes the downward part of the QBO, the QBO oscillation slows down. Figuratively, one can assume a child running upward on a downward moving escalator, which is less successful the faster the escalator is.

3 Description model and simulations

3.1 Model setup

The simulations for this study were performed with the middle atmosphere version of the general circulation model (GCM) ECHAM5 (Giorgetta et al., 2006), using the spectral truncation at wavenumber 42 (T42) and 90 vertical layers up to 0.01 hPa. The GCM solves prognostic equations for temperature, surface pressure, vorticity, divergence, and phases of water. In this model version with 90 vertical levels the quasi-biennial oscillation (QBO) in the tropical stratosphere is internally generated (Giorgetta et al., 2006).

The aerosol microphysical model HAM (Stier et al., 2005) is interactively coupled to the GCM. HAM calculates the sulfate aerosol formation including nucleation, accumulation, condensation and coagulation, as well as its removal processes by sedimentation and deposition. A simple stratospheric sulfur chemistry is applied above the tropopause (Timmreck, 2001; Hommel et al., 2011). The sulfate is radiatively active for both, SW and LW radiation, and HAM is coupled to the radiation scheme of ECHAM5. The sulfate aerosol influences dynamical processes via temperature changes caused by scattering of solar radiation and absorption of near-infrared and infrared radiation. Within this stratospheric HAM version apart from the injected $\mathrm{SO_2}$, only natural sulfur emissions are taken into account. These simulations use the model setup described in Niemeier et al. (2009) and Niemeier and Timmreck (2015). The sea surface temperature (SST) is set to a climatological values as in Toohey et al. (2011) and does not change due to CE.

3.2 Simulations

We estimate the impact of changes of the QBO phase on transport via varying the injection-rate, -height and -area. We inject 4, 6, 8 and 10 $\mathrm{Tg(S)yr^{-1}}$ at heights of 60 hPa and 30 hPa (19 km and 24 km). Injection rates of 4 and 8 $\mathrm{Tg(S)yr^{-1}}$ were chosen to study the impact of the heated aerosol layer on the QBO, as well as the feedback of the changing dynamics on the transport of sulfate. The simulation with an injection of 4 $\mathrm{Tg(S)yr^{-1}}$ allows us to build composites of different QBO-phases to get a direct comparison of their impact on transport. Simulated results using injection rates with 8Tg(S)/y and 10 $\mathrm{Tg(S)yr^{-1}}$ are in general similar because the QBO breaks down in both cases.

Atmos. Chem. Phys. Discuss., doi:10.5194/acp-2017-470, 2017
Manuscript under review for journal Atmos. Chem. Phys.
Discussion started: 29 May 2017

Natural variation is high in the tropics due to the different QBO phases and also at high latitudes due to a very variable polar vortex. Both reduces the statistical significance of the results and requires long simulation periods. Therefore,when discussing dynamical impacts in Section 4 and Section 5 we base this on the long simulations 8Tg60 and 8Tg30 (Table 1), extended over 40 and 30 years, respectively.

The $10\,\mathrm{Tg(S)yr^{-1}}$ simulations (10Tg60, 10Tg30 and 10Tg60lat30) with a length of 10 years (Table 1) have been performed in order to allow a comparison to results in Niemeier and Timmreck (2015). We show their simulation result (Geo10), which was performed with a 39 level version of ECHAM5-HAM, without internally generated QBO. This allows a direct comparison of the impact of the model resolution and resulting different tropical wind profiles on the results (Section 6). Most simulations were performed with injections into one grid box at the equator. We performed also a simulation were we extend the injection area to a band between 30° N and 30° S (10Tg60lat30) with the same zonal extension and position as the box (Table 1). This reduces the amount of sulfur injected in the tropics and reduced the radiative heating. However, Niemeier and Timmreck (2015) showed that this strategy intensifies meridional transport and reduces the forcing efficiency.

All anomalies are calculated relative to the control simulation. Without sulfur injections, this simulation generates a QBO with an average period of about 32 month. Thus, all averages over the timeseries contain both QBO phases. Results in Sections 4 and 5 are are averaged over the period given in Table 1. Results in Section 6 are averaged over the last three (Geo10) or four years of the simulation.

Table 1. Overview of the parameters for the simulations performed with ECHAM5-HAM. The injection rate differs between the simulations, as well as injection-area and -height. *Box* is one grid box at the equator at 120.9° E to 123.75° E and equator to 2.8° N. The injection area *30° N to 30° S* has in longitudinal direction also the width of one grid box. The globally averaged aerosol optical depth (AOD) is given for comparison purposes.

Simulation name	Injection rate	Injection height	Injection area	Number of vert. levels	Simulation duration	AOD
4Tg60	$4\,\mathrm{Tg(S)yr^{-1}}$	60 hPa	box	90	50 y	0.085
4Tg30	$4\,\mathrm{Tg(S)yr^{-1}}$	30 hPa	box	90	20 y	0.089
8Tg60	$8\,\mathrm{Tg(S)yr^{-1}}$	60 hPa	box	90	40 y	0.13
8Tg30	$8\,\mathrm{Tg(S)yr^{-1}}$	30 hPa	box	90	30 y	0.12
10Tg60	$10\,\mathrm{Tg(S)yr^{-1}}$	60 hPa	box	90	10 y	0.151
10Tg30	$10\,\mathrm{Tg(S)yr^{-1}}$	30 hPa	box	90	10 y	0.131
10Tg60lat30	$10\,\mathrm{Tg(S)yr^{-1}}$	60 hPa	30° N to 30° S	90	10 y	0.157
Geo10	$10\,\mathrm{Tg(S)yr^{-1}}$	60 hPa	box	39	6 y	0.176
Control	$0\,\mathrm{Tg(S)yr^{-1}}$			90	50 y	

Atmos. Chem. Phys. Discuss., doi:10.5194/acp-2017-470, 2017
Manuscript under review for journal Atmos. Chem. Phys.
Discussion started: 29 May 2017

Atmospheric Chemistry and Physics
Open Access
Discussions

4 Implication of sulfur injection for stratospheric dynamics

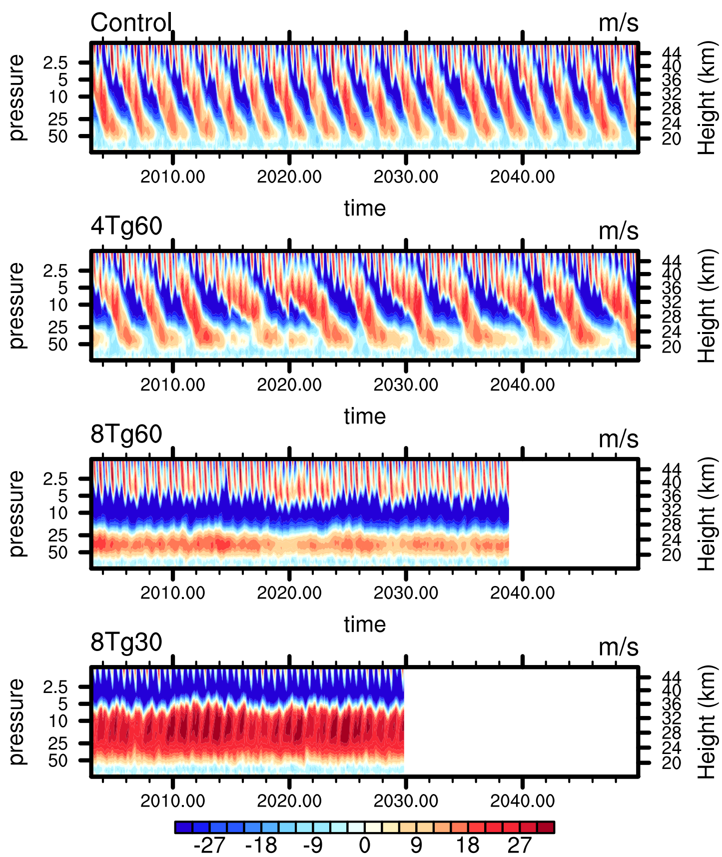

Figure 1. Zonal mean zonal wind velocity ms^{-1} at the equator for the control simulation and simulations with injection rates of $4\,\mathrm{Tg(S)yr}^{-1}$ and $8\,\mathrm{Tg(S)yr}^{-1}$ at a height of $60\,\mathrm{hPa}$ and $8\,\mathrm{Tg(S)yr}^{-1}$ at $30\,\mathrm{hPa}$.

The injection of sulfur into the stratosphere and the resulting heating by the aerosols causes a change of the QBO frequency in our simulations (Fig. 1). The results are similar to Aquila et al. (2014) but in their simulations the QBO is impacted at lower injection rate. Different to Aquila et al. (2014) we use a full aerosol microphysical model and simulate the evolution of the aerosol with varying particle sizes. Injecting $4\,\mathrm{Tg(S)yr}^{-1}$ at $60\,\mathrm{hPa}$ causes a prolongation of the westerly phase in the lower stratosphere (70 to $25\,\mathrm{hPa}$). The downward propagation of the easterly winds above $25\,\mathrm{hPa}$ is delayed by several month. Injecting $8\,\mathrm{Tg(S)yr}^{-1}$ has the consequence of a complete shutdown of the oscillation. In the lower stratosphere, between $50\,\mathrm{hPa}$ and $25\,\mathrm{hPa}$ a layer with

Atmos. Chem. Phys. Discuss., doi:10.5194/acp-2017-470, 2017
Manuscript under review for journal Atmos. Chem. Phys.
Discussion started: 29 May 2017

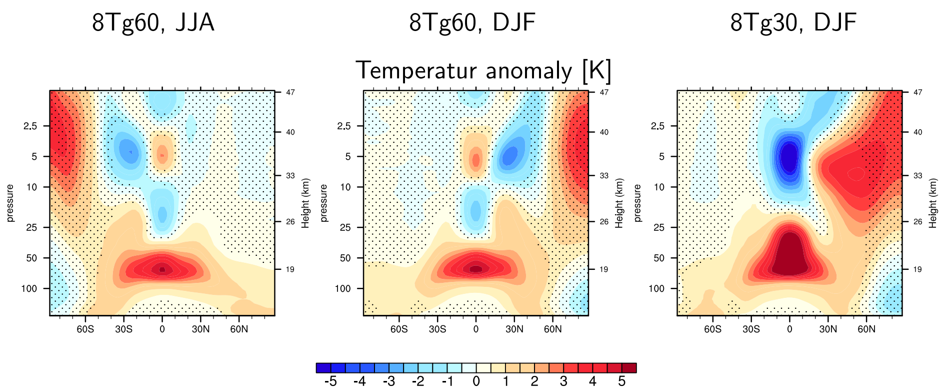

Figure 2. Zonal mean temperature anomaly for injection of 8 $\mathrm{Tg(S)yr^{-1}}$ at 60 hPa (left and middle) relative to control run at northern hemisphere summer (JJA, left) and winter (DJF, right) and DJF for an injection at 30 hPa. Results are compared to a control simulation which includes different phases of the QBO. Stippling indicates areas which are not significant at the 95% level.

constant westerly winds develops, accompanied by a layer of constant easterly winds above. When injecting at 60 hPa the semi-annual oscillation (SAO) in the upper stratosphere propagates down to 5 to 10 hPa, comparable to the control simulation. Injection of 8 $\mathrm{Tg(S)yr^{-1}}$ at higher level, 30 hPa, intensifies the westerly jet in strength and increases its vertical extension (up to 5 hPa). The easterly jet and the lower limit of the SAO region are shifted upward. A new feature is the apparent upward propagation of the westerly wind maximum in the based westerly jet with a frequency of one year.

4.1 Effects on stratospheric temperature

We discuss the temperature and wind anomalies for simulations with an injection rate of 8 $\mathrm{Tg(S)yr^{-1}}$ (Fig. 2 and Fig. 3): injection at 60 hPa for southern hemispheric winter (JJA) and northern winter (DJF) and for DJF for an injection at 30 hPa. The anomalies are relative to the mean over the 50 year control simulation which includes all phases of the QBO.

The broad temperature anomaly in the lower stratosphere is caused by the absorption of LW radiation through sulfate and, thus, reflects the position of the aerosol layer (Fig. 2). The strongest warming, between 30° N to 30° S and 50 hPa to 100 hPa, occurs just below the maximum sulfate concentration. The positive anomaly does not extend to the pole in the winter hemispheres, because the polar vortexes block the transport of the aerosols. This temperature anomaly in the heated sulfate layer is significant at the 95% level, calculated using a Student t-test. Above this heated layer the typical temperature pattern with anomalies of opposite sign at the equator and in the subtropics

Atmos. Chem. Phys. Discuss., doi:10.5194/acp-2017-470, 2017
Manuscript under review for journal Atmos. Chem. Phys.
Discussion started: 29 May 2017

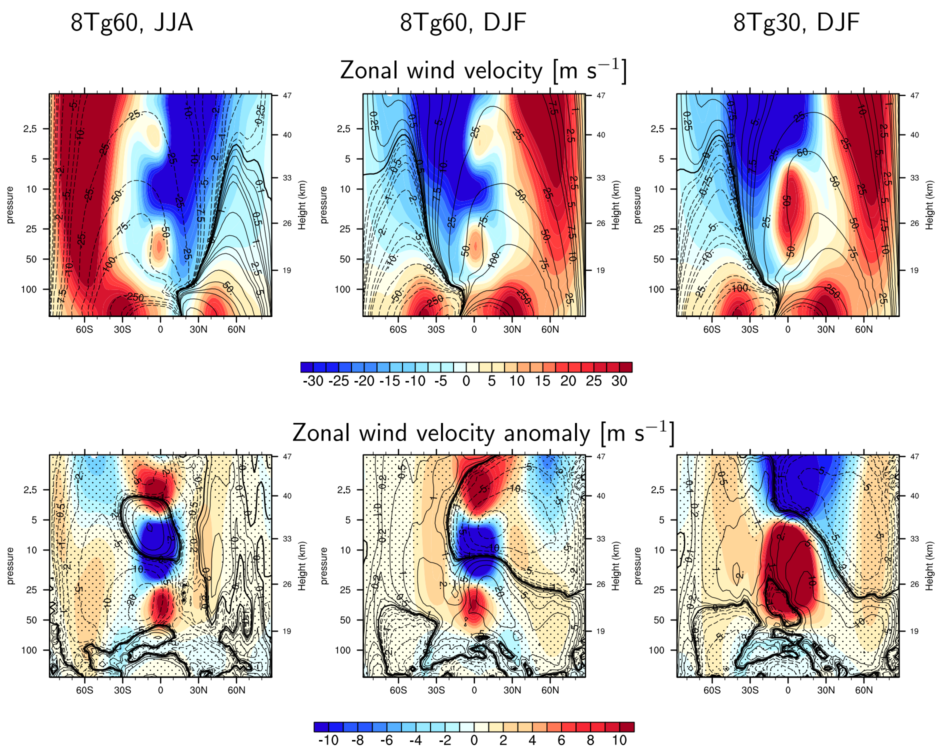

Figure 3. Zonal mean zonal wind velocity (top) and the anomaly of the zonal wind velocity (bottom) for injection of $8\,\mathrm{Tg(S)yr^{-1}}$ at $60\,\mathrm{hPa}$ (left and middle) relative to control run at northern hemisphere summer (JJA, left) and winter (DJF, middle) and DJF for an injection at $30\,\mathrm{hPa}$ (right). Contour lines show the stream function [kg s^{-1}] (top) and the difference of the streamfunction to the control simulation (bottom) for the two seasons. Results are compared to a control simulation which includes different phases of the QBO. Stippling indicates areas which are not significant at the 95% level.

appears, related to the secondary meridional circulation (SMC) of equatorial jets, here as a result of the change in the mean wind structure. In our results theses signals are significant in the winter hemisphere, e.g. JJA at 30°S at $20\,\mathrm{hPa}$ and $5\,\mathrm{hPa}$, opposite to the positive anomaly of more than 3°K at the winter pole. Internal variability around the polar vortex is too high to allow significant results with timeseries of only 30 and 50 years.

Injecting at $30\,\mathrm{hPa}$ (8Tg30) results in a vertically thicker aerosol layer. The sedimentation path is longer and the aerosol is injected into an area were the tropical pipe dominates and meridional transport is lower than in 8Tg60 (see Section 2). Therefore, in 8Tg30 the heating of the sulfate aerosol extends up to a height of 25 hPa. We also get a warming at 30° N, where we get a negative anomaly in 8Tg60. A consequence is a reduction of the equator to pole temperature gradient in the upper stratosphere, and an increase of the gradient in the lower stratosphere.

4.2 Effects on zonal and meridional wind

A dominating feature of the zonal winds are the polar night jets (Figure 3, top). The velocity in the tropical jets of the QBO, in Control as well as in 8Tg60, is about a factor of three smaller than in the polar night jet. This changes when injecting at 30 hPa (8Tg30). The velocity is comparable to the velocity of the polar jet at a similar altitude. Also the vertical extension of the jet increases to a height of 5 hPa. The vertical extension of the jet is coupled to the temperature by the SMC, causing a cooling and warming above and below, respectively, the level with maximum wind, ca. at 25 hPa. Therefore, the changes in the QBO winds, caused by the heating of the sulfate layer in the lower stratosphere, extend the temperature anomalies into the upper stratosphere to fulfill the thermal wind balance. In 8Tg30 the westerly jet is much wider than in 8Tg60 and, additionally, broadens towards the winter hemisphere. The westerly component of the wind anomaly is intensified far into the subtropics. This might be related to wave propagation as described in Section 2.2. A detailed analysis is beyond the scope of this paper.

In both simulations the summer easterlies are weakened around 30°, the only significant impact of the sulfate on the zonal wind outside of the tropics. The polar night jet partly intensifies in lower stratosphere of 8Tg60 and intensifies and is pushed poleward in 8Tg30. However, a not significant signal.

4.3 Effects on the Brewer Dobson Circulation

The black contours in Fig. 3 (top) show isolines of the mass stream-function. Positive streamlines describe clockwise motion, negative (dashed) ones counter-clockwise motion. The streamlines represent the BDC with the overturning circulation in the winter hemisphere, but they do not show wave induced mixing in the surf-zone and transport barriers (Haynes and Shuckburgh, 2000). The contour lines in Fig. 3 (bottom) show the anomaly of the streamlines with respect to the control simulation. Dashed lines indicate negative anomalies which would be an intensification of counter-clockwise motion. Continuous anomaly lines are positive.

Compared to the control run (anomaly in Fig. 3, bottom) this vertical transport is intensified in both simulations at the equator up to 10 hPa in 8Tg60. But the streamline rises higher in 8Tg30 which indicates the increased vertical motion in the westerly jet in 8Tg30. The downward motion at the winter pole intensifies only at the South Pole through the whole stratosphere, not at the North Pole, where we cannot confirm the results of Aquila et al. (2014). They show qualitatively an intensification of the vertical and meridional flow above 10 hPa. Our results show an intensification of the flow below 10 hPa, related to the westerlies, and reduced values of the stream function for

Atmos. Chem. Phys. Discuss., doi:10.5194/acp-2017-470, 2017
Manuscript under review for journal Atmos. Chem. Phys.
Discussion started: 29 May 2017

the easterlies in the upper stratosphere. This difference should have consequences for the transport of species like ozone, which are not calculated in this study. However, the streamlines do not represent wave induced meridional mixing (Butchart, 2014). We show in section 5 that also the quasi horizontal mixing is important for the transport of sulfate.

5 Implication of changes in stratospheric dynamics on the distribution of sulfate

In this section we discuss the relation between the dynamical changes in the QBO and the distribution of sulfate. We discuss how transport and sulfate distribution depend on the QBO phases in section 5.1 and indicate an impact of the injection rate on transport of sulfate in section 5.2.

5.1 Impact of the QBO phases on sulfate distribution

Simulation 4Tg60 shows still periods with easterly winds in the lower stratosphere at the equator. This allows to examine the differences in transport between different QBO phases. Our definition of QBO phase composites differs from usual definitions in the literature. The aim was to get clear signals in very different composites which cover main characteristics of the equatorial jets under CE. We apply the composite criterion for each month of the timeseries and calculated a multi-year monthly mean for each composite:

- Comp West: Westerly winds stronger than 10 m/s at 20 hPa. This composite covers situations in undisturbed QBO and is also close to the situation in 8Tg30.
- Comp East: Westerly winds stronger than 8 m/s at 50 hPa and easterly at 20 hPa. This composite covers many of the westerly tails in 4Tg60 and the jets in 8Tg60.

In the tropics the meridional distribution of sulfate concentration is broader for Comp West with less vertical extension than in Comp East (vertical cross section in Fig. 4, top), illustrated also by negative anomalies above 50 hPa in the difference plot. The anomalies show higher concentrations in mid and high latitudes in Comp West which indicates stronger meridional transport. The reason is twofold: wave propagation and different ω^*. Following Haynes and Shuckburgh (2000), within westerly QBO winds waves are able to propagate across the equator and break, causing mixing, on the summer side of the westerlies. This results in more meridional mixing across the subtropical transport barrier. Additionally, the residual vertical velocity ω^* (Fig. 4, bottom) is larger for Comp East around 25 hPa, an area related to the easterly shear zone. This is in agreement with the vertical transport described in Plumb and Bell (1982) for easterly shear. This easterly shear zone overlaps in Comp East with the sulfate layer, which explains the larger vertical extension of sulfate in Comp East. In Comp West the maximum vertical velocity is even stronger but is located above 10 hPa an area with low sulfate concentrations.

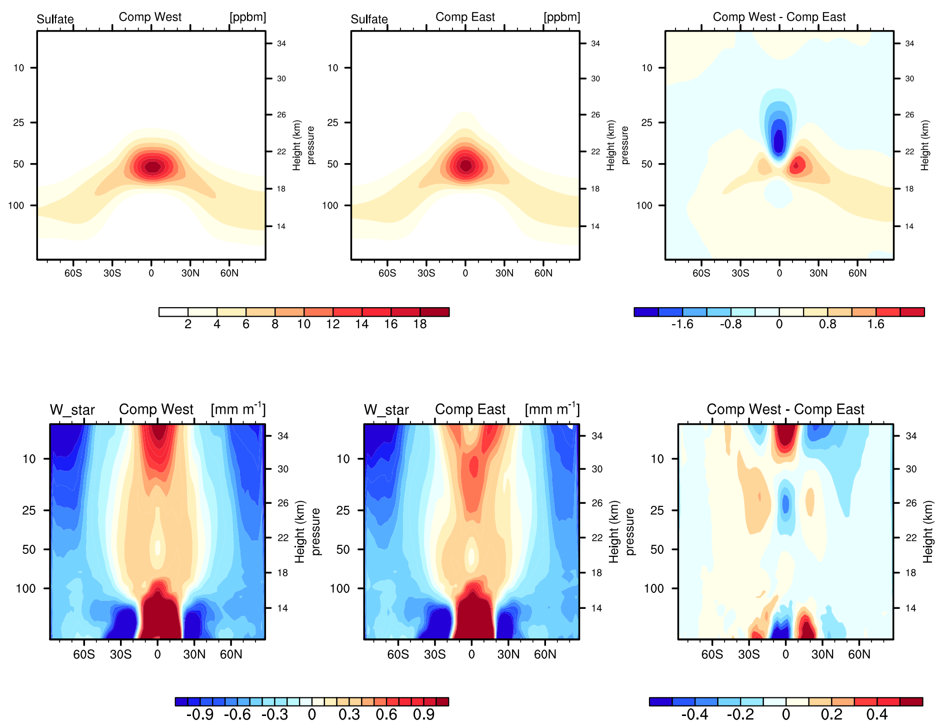

Figure 4. Top: Zonal mean of sulfur concentration [ppbm] for $4\,\mathrm{Tg(S)yr^{-1}}$ injected at $60\,\mathrm{hPa}$ for Composite West (left), Composite East (middle) and difference of Composite W - Composite E (right). Bottom: Zonally averaged residual vertical velocity ω^* for both composites and the difference.

Figure 5 (left) shows the normalized sulfate burden, the vertical integral of the SO_4 concentration per area, of the two composites as well as the difference of both (right). The data are normalized by division with the corresponding injection rate. The normalized tropical burden values are slightly lower in Comp West, while the extratropical burden is higher. We note an asymmetry in the meridional transport between the hemispheres with up to 20% higher burden in the northern hemisphere in Comp West. We currently do not have an explanation for this asymmetry but it is most probably related to the wave propagation described above, which is stronger in the northern hemisphere.

5.2 Effects on sulfate burden

The Hovmøller diagram of the normalized sulfate burden (Fig. 6, A) shows slightly different patterns of sulfate distribution for the different injection scenarios. All four simulations in common is a maximum in the tropics and intra-seasonal variations in the extratropics. Sulfate is accumulated between 40° and 60° in the winter hemisphere because the winter polar vortex blocks the transport

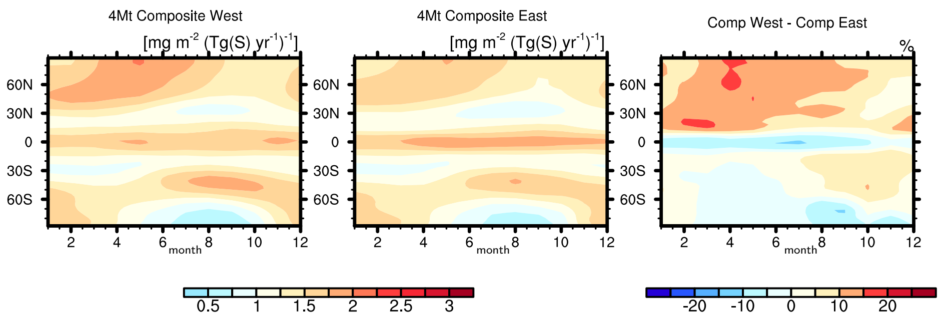

Figure 5. Zonal and multi-year monthly means of normalized SO_4 burden $[\mathrm{mg\,m^{-2}(Tg(S)\,yr^{-1})^{-1}}]$ of simulation 4Tg60 plotted as Hovmøller diagram. Left: Composite West, Middle: Composite East, and Right: the difference of both in percent.

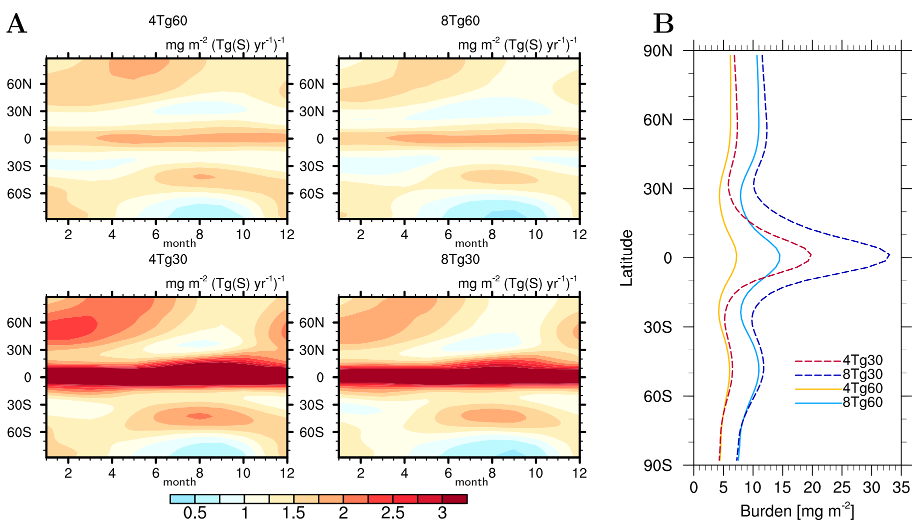

Figure 6. A: Hovmøller diagram of normalized zonally averaged monthly mean sulfate burden $(\mathrm{mgm^{-2}(Tg(S)yr^{-1}})$ for injection rates of $4\,\mathrm{Tg(S)yr^{-1}}$ (left) and $8\,\mathrm{Tg(S)yr^{-1}}$ (right) and an injection heights of $60\,\mathrm{hPa}$ (top) and $30\,\mathrm{hPa}$ (bottom). To normalize the data each field is divided by the injection rate. B: Zonally averaged non-normalized sulfate burden.

until solar heating breaks down the vortex. In general, in mid and high latitudes the normalized burdens are larger in the $4\,\mathrm{Tg(S)yr^{-1}}$ scenarios than in the 8 Tg scenarios. Thus, meridional transport decreases with increasing injection rate. 4Tg60 is an average over the timeseries and includes Comp

West and Comp East. 8Tg60 has a clear tropical maximum and lower normalized burden in mid- and high-latitudes than 4Tg60. The vertical structure of the tropical winds is similar in 8Tg60 to Comp East. The differences between the burden patterns are similar to the ones in Figure 5. Thus, the differences to 4Tg60 can again be explained by wave propagation and different ω^*.

Obvious are the differences between the two injection heights. When injecting at 30 hPa the tropical maximum increases compared to the 60 hPa injection height simulations and high sulfate burden covers a wider area in the tropics: 20° N to 20° S instead of 12° N to 12° S. Also the non-normalized zonally averaged burden (Fig.6, B) shows for the 30 hPa cases higher values in the subtropics, related to the wider jet. Additionally, the subtropical minimum moves poleward (Fig.6, B) while in the mid and high latitudes the non-normalized burden values are similar to the lower injection case. Thus, the increase in injection height results in stronger burden mainly in the tropics and sub-tropics. This differs from previous results, using a model with lower vertical resolution, where an increase in injection height results in globally higher burden (Niemeier et al., 2011). We discuss the impact of these differences on radiative forcing in Section 6.

Increasing the injection level in simulations 4Tg30 and 8Tg30 extends the sulfate layer vertically. The westerly jets extend almost up to 5 hPa making the conditions comparable to Comp West. (The tropical jets of 4Tg30 are similar to 8Tg30, but with lower velocity.) Thus, wave propagation increases meridional transport compared to 8Tg60 in the same way as between Comp West and Comp East and explains the poleward shift of the subtropical minimum. Punge et al. (2009) show that the concentration gradient in the subtropics is smaller in the summer hemisphere during the westerly phase. This causes mixing of sulfate into the sub-tropics which is mixed further poleward in autumn and results in slightly higher concentrations and burdens in mid-latitudes in 4Tg30 and 8Tg30 compared to the lower injections height. However, this process is small compared to the much stronger increase in normalized tropical sulfate burden where both simulations show a strong maximum. The increased temperature anomaly (Fig. 2) intensifies the tropical jet. As described for the polar jets, a jet creates a transport barrier and the strong tropical westerly jet acts as a strong transport barrier. The stronger the jet, the stronger the barrier. Thus, both, stronger wave activity and stronger barrier, coexist.

Here we can identify a classical feedback loop: The stronger the injection, the stronger the warming, which increases via the thermal wind imbalance the zonal wind velocity. The stronger wind increases the transport barrier which keeps more $\mathrm{SO_4}$ within the tropics. This results in an even higher heating. Additionally, the results highlight the importance of quasi-horizontal mixing for the distribution of the surface aerosol. Transport in the BDC would be less sensitive to a stronger subtropical transport barrier.

Atmos. Chem. Phys. Discuss., doi:10.5194/acp-2017-470, 2017
Manuscript under review for journal Atmos. Chem. Phys.
Discussion started: 29 May 2017

Atmospheric Chemistry and Physics Discussions

6 Implications of changes in stratospheric sulfate transport for radiative forcing

We have shown that radiative heating of the sulfate aerosols impacts the quasi biennial oscillation by slowing or even shutting down the oscillation. In turn, the changed QBO impacts the meridional transport of the sulfate. What does this mean for the efficiency of CE? A good measure for the efficiency is the TOA radiative forcing. This value is necessary to calculate the amount of SO_2 needed to counteract a certain amount of greenhouse forcing (Niemeier et al., 2013) and, therefore, determines the efficiency of a sulfur injection. In this study the TOA forcing of sulfate is calculated as the difference between the active radiative forcing with aerosols and the diagnostic radiative forcing without aerosols, which results from doubled radiative transfer calculations (see also Niemeier and Timmreck (2015)).

We performed simulations with an injection rate of $10\,\mathrm{Tg(S)yr^{-1}}$ in order to allow direct comparison to the results of Niemeier and Timmreck (2015). They used ECHAM5-HAM in a 39-layer version that would not allow for an internally generated QBO, simulating instead constant equatorial easterly winds. This allows us to roughly estimate an error in the sulfate forcing made by using a dynamically too simple model. Mean wind velocities in the westerly jet increases by 5% (10Tg60) and 10% (10Tg30), respectively, compared to the 8Tg cases shown in Figure 1.

6.1 Effects on aerosol radiative properties

The sulfate burden of the three simulations, given in Figure 7, is similar in the extratropics, while the results of the vertically integrated aerosol optical depth (AOD) differ between the simulations. So we may assume that the burden is less sensitive to changes in the tropical wind systems than the AOD, which depends not only on the sulfate mass but also on the particle number.

The comparison of simulation Geo10, low resolution model version without internally generated QBO, and simulation 10Tg60 shows in tropics and sub-tropics the impact of the different subtropical transport barriers. The constant easterly winds in Geo10 cause a more permeable barrier (Punge et al., 2009) resulting in a stronger meridional transport. The model version with lower vertical resolution tends to overestimate meridional transport, a tendency seen in earlier volcano studies (Niemeier et al. (2009), Timmreck et al. (1999)).

A clear effect is the roughly 20% lower AOD in 10Tg60 compared to Geo10 outside of the tropics with similar burden values in this region. The particle number density of Geo10 is larger in the accumulation mode and lower in the coarse mode (Figure 8). This larger number of small particles results in more scattering. In other words, the strong jet in 10Tg60 keeps the aerosols in the tropics. The particles grow larger and scatter less.

Increasing the injection height to $30\,\mathrm{hPa}$, simulation 10Tg30, further intensifies the equatorial westerly jet. Thus, the subtropical transport barrier is strengthened resulting in a very strong maximum of burden and AOD in the tropics, as discussed in Section 5.2. In the extratropics the AOD

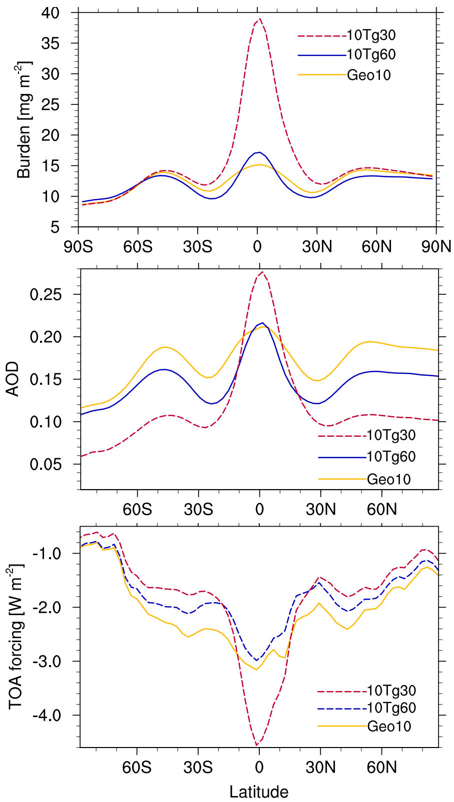

Figure 7. Zonal mean sulfate burden (top), aerosol optical depth at 550 µm (middle) and top of the atmosphere forcing (bottom) for different experiments with $10\,\mathrm{Tg(S)yr}^{-1}$.

is 30% to 50% lower compared to simulation 10Tg60. Figure 8 indicates low meridional transport, resulting in low particle number densities in the extratropics in 10Tg30. Due to the confinement of the particles in the tropics grow particles to larger size. The reduction in the extratropics is strong enough to reduce the global mean AOD of 10Tg30 compared to 10Tg60 (Tab. 1).

6.2 Effects on radiative forcing

Niemeier and Timmreck (2015) have shown that the global TOA radiative forcing depends on the meridional distribution of aerosols. Models which simulate a stronger transport barrier (e.g. English et al. (2012)) show lower TOA forcing per injected amount of sulfur. So the increased tropical transport barrier and decreased AOD in the extratropics in simulations with internally generated QBO and the described shift of particle size toward coarse mode particles should change the forcing efficiency, the relation of TOA radiative forcing to injection rate, discussed in Niemeier and Timmreck (2015).

Atmos. Chem. Phys. Discuss., doi:10.5194/acp-2017-470, 2017
Manuscript under review for journal Atmos. Chem. Phys.
Discussion started: 29 May 2017

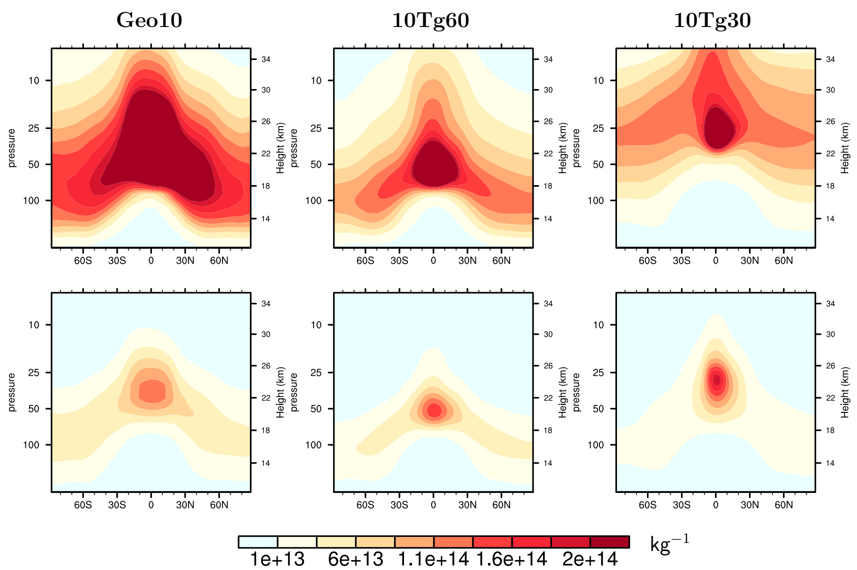

Figure 8. Zonal mean of aerosol number density [kg^{-1}] for experiments Geo10 (left), 10Tg60 (middle), and 10Tg30 (right) with an injection rate of $10\,\mathrm{Tg(S)yr^{-1}}$ with and without QBO. Top: Accumulation mode particles with a size of $0.05\,\mu\mathrm{m} \leq r \leq 0.2\,\mu\mathrm{m}$. Bottom: Coarse mode particles ($r \geq 0.2\,\mu\mathrm{m}$). Only particles in accumulation and coarse modes are radiatively active.

The zonal mean of TOA radiative forcing is smaller in simulation 10Tg60 than in Geo10 (Figure 7, bottom), even close to the equator, where the AOD of 10Tg60 is slightly larger. This is again the impact of the shift to larger particles.

Comparing the global TOA forcing (Figure 9) of sulfate of this study (XTg60, blue line) to simulations with lower vertical resolution (GeoX, orange line) of Niemeier and Timmreck (2015) the slope of the blue curve is smaller. Thus, the efficiency of the sulfur injection with increasing injection rate decreases stronger than described in Niemeier and Timmreck (2015). While forcings are very similar for lower emission rates, for injection rates above $10\,\mathrm{Tg(S)yr^{-1}}$ the forcing in the XTg60 simulations is 10% to 13% lower. This would require even stronger injection amounts to counteract a certain greenhouse gas forcing.

In previous studies, the efficiency increased when the injection height was increased. In Niemeier and Timmreck (2015) TOA forcing increases by 50% for an injection of $10\,\mathrm{Tg(S)yr^{-1}}$. In this study TOA forcing of 8 Tg30 increases only by 18% and by 8% for 10Tg30 compared to 4Tg60 and 10Tg60, respectively. The efficiency even decreases for strong injection rates of $20\,\mathrm{Tg(S)yr^{-1}}$ and more, a consequence of the strong dynamical changes in the high injection cases. This result

Atmos. Chem. Phys. Discuss., doi:10.5194/acp-2017-470, 2017
Manuscript under review for journal Atmos. Chem. Phys.
Discussion started: 29 May 2017

Atmospheric Chemistry and Physics
Open Access
Discussions

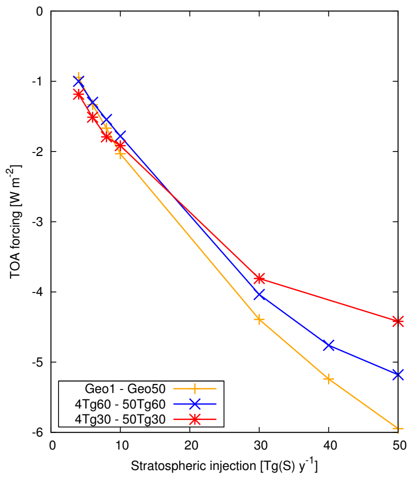

Figure 9. Injection rate against globally averaged top of the atmosphere radiative forcing (all sky) for simulations with low vertical resolution (GeoX) and high vertical resolution and two injection heights (XTg60 and XTg30).

challenges an injection at 30 hPa in general, because this injection height is technically much more demanding.

6.3 Effects of wider injection area

To avoid the strong impact of the sulfate radiative heating on the QBO the injection area was increased to a band between 30° N and 30° S (10Tg60lat30). Injecting partly into the surf-zone increases meridional transport and reduces the amount of sulfur injected in the tropics. This reduces the impact on the QBO and causes no longer a complete shut down of the QBO but an extended period of the oscillation of roughly five years (Fig. 10).

This simulation results in lower AOD in the tropics, but up to 50% higher values in the extratropics compared to 10Tg60 (Fig. 11, left). The maximum of the AOD is shifted into the extratropics because of the increased meridional transport. The resulting radiative forcing has its maximum around 40° S (Figure 11, right), thus, stronger transport into the southern hemisphere. 10Tg60lat30 simulates long periods with easterly shear (Figure 10), similar to the conditions of Comp East, which also result in stronger transport into the southern hemisphere (Figure 5).

Extending the injection area reduces the impact on the QBO with the side effect of the decreased forcing in the tropics and increased forcing in midlatitudes. A further increase of the injection area would likely strengthen this effect. Another option would be to inject poleward of ±15°. This would leave the tropics with much lower reduction in solar forcing because almost no extratropical air

Atmos. Chem. Phys. Discuss., doi:10.5194/acp-2017-470, 2017
Manuscript under review for journal Atmos. Chem. Phys.
Discussion started: 29 May 2017

Atmospheric Chemistry and Physics Discussions

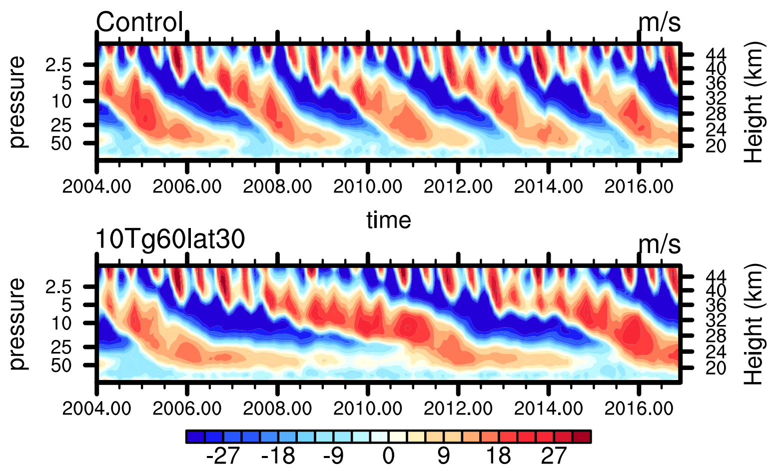

Figure 10. Zonal mean zonal wind velocity at the equator for the control simulation and for an injection of 10 Tg(S)yr^{-1}r between 30° N and 30° S.

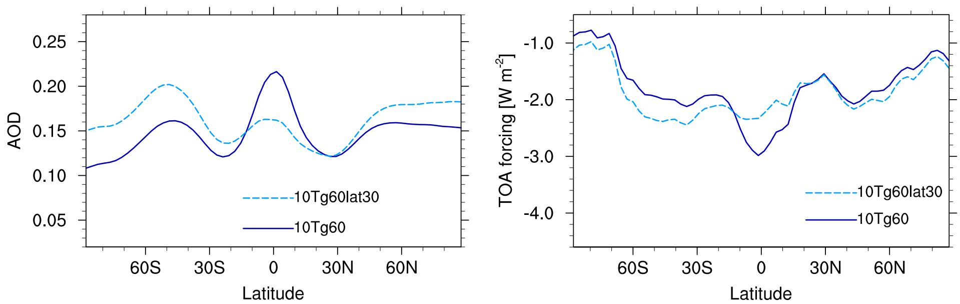

Figure 11. Aerosol optical depth at 550 µm (left) and top of the atmosphere forcing (right) for an experiment with injections between 30° N and 30° S (10Tg60lat30) and 10Tg60.

is directly mixed into the tropics in the stratosphere (O'Sullivan and Chen, 1996), only by wave induced mixing as described in Section 5. Laakso et al. (2017) found 40% lower solar forcing in the tropics when injecting at 15° from the equator compared to an equatorial injection. We showed that the meridional transport depends on the impact of the sulfate heating on the equatorial winds in the tropical stratosphere. Thus, the injection strategy may play an important role in the global distribution of the sulfate aerosol. The climatic impact of the aerosol distribution in 10Tg60lat would differ from previous studies with a globally more even CE forcing distribution.

Atmos. Chem. Phys. Discuss., doi:10.5194/acp-2017-470, 2017
Manuscript under review for journal Atmos. Chem. Phys.
Discussion started: 29 May 2017

Atmospheric Chemistry and Physics
Open Access
Discussions

7 Conclusions

The results of this study show a strong impact of the absorption of infrared radiation by sulfate and the related additional warming in the stratosphere on the dynamics and transport processes in this region. Our results differ in detail from Aquila et al. (2014) but confirm their results on the impact of the stratospheric heating on the QBO phases. The dynamical state of the stratosphere determines the transport of species from the tropics into the extratropics. Strong equatorial jets hinder transport and confine the sulfate in the tropics. Strong westerly jets develop at the equator in the stratosphere in our simulations for injections of 6 $\mathrm{Tg(S)yr^{-1}}$ and more. The edge of the jet, where winds become easterly, is a transport barrier which gets stronger with increasing wind velocity. The consequence is low meridional transport out of the tropics and a decreased AOD and TOA forcing in the extratropics. Moderate westerly winds in the tropics at the height of the sulfate layer cause stronger transport towards the northern hemisphere (Section 5.1). Easterlies or westerly shear, as e.g. dominating in the wider injection case (10Tg60lat30), cause stronger transport towards the southern hemisphere (Section 6.3). We assume the reason is stronger wave propagation thought the tropics into the subtropics in westerly winds (Section 5.1). This different stratospheric transport would impact also dynamical processes and the hydrological cycle in the troposphere. Haywood et al. (2013) describe e.g. a strong shift of the position of the ITCZ when shielding only one hemisphere via a sulfate layer, which is likely after an extra-tropical volcanic eruption.

A vertically extended sulfate layer results from injections at 30 hPa. The consequence is a strong westerly jet, which extends high into the stratosphere (5 hPa). This reduces meridional transport in our strong and high level injection case (10Tg30) to a point that CE would impact almost only the tropics and subtropics. Previous simulations indicated a strong increase of AOD and TOA radiative forcing (up to 50%) when increasing the injection height (English et al. (2013), Niemeier and Timmreck (2015)). In this study we got only a a small increase of 18% for 4 $\mathrm{Tg(S)yr^{-1}}$, of 8% for 10 $\mathrm{Tg(S)yr^{-1}}$ and even less forcing than the lower injection height for strong injections. Both previous studies were performed with models not simulating the QBO. This shows the importance a realistic representation of equatorial dynamics in particular of the QBO for the QBO relevant transport patterns in transport studies like CE, impact of volcanoes, and studies of stratospheric chemistry. A conclusion from this results can be that injecting at 30 hPa is no longer an option for CE, especially as it is technically more demanding.

The simulations in this study do not include stratospheric chemistry. Therefore, we can not describe the impact of the dynamical changes in the stratosphere on other species like ozone. Ozone would be impacted twofold: via chemical reactions related to sulfur chemistry and via changed transport. Thus, the described reduction in meridional transport of sulfate may also be true for ozone and the stratospheric ozone concentration could be reduced in the extratropics. This reduction would add to the proposed reduction of ozone due to chemical reactions (Tilmes et al., 2008).

An additional caveat is the fact that we have not changed the sea surface temperature in this study. Estimated from GeoMIP simulations (Niemeier et al., 2013) CE with an injection of $6\,\mathrm{Tg(S)yr^{-1}}$ would roughly cause a decrease of the sea surface temperature of one degree . This impacts convection which then modifies the generation of gravity waves and likely the period of he QBO. More detailed answers will be left for future studies.

In this study we calculated a smaller efficiency of sulfur injections than Niemeier and Timmreck (2015). Therefore we have to adapt some of the conclusions drawn in Niemeier and Timmreck (2015). They estimated that an injection of $45\,\mathrm{Tg(S)yr^{-1}}$ could keep the global mean temperature at 2020 level until 2100 while maintaining business as usual emissions. Following this study, $70\,\mathrm{Tg(S)yr^{-1}}$ would be the lowest estimate to keep this temperature level. Increasing the injection height would even increase the require injection rate. Estimates of the cost and feasibility of CE depend also on the forcing efficiency. Moriyama et al. (2016) estimate from the results of the study of Pierce et al. (2010) that it would be necessary to operate 1300 planes to decrease radiative forcing through sulfur injections by $2\,\mathrm{Wm^{-2}}$, or 6700 flight per day (personal communication). Pierce et al. (2010) required $3\,\mathrm{Tg(S)yr^{-1}}$ (as H_2SO_4) to get $2\,\mathrm{Wm^{-2}}$. The new results of this study show that with ECHAM5-HAM even $10\,\mathrm{Tg(S)yr^{-1}}$ would not be enough, $12\,\mathrm{Tg(S)yr^{-1}}$ might be necessary. Thus, a factor of 4 more planes and flights would be required than in the study of Moriyama et al. (2016).

Finally, it needs to be stated that the simulated impact of stratospheric sulfate heating on the QBO is only a model result which cannot be proved in reality. However our simulations show that the efficiency of sulfur injections may depend crucially on the jet structure in the tropical stratosphere, which itself will be influenced strongly by the injections. Our simulations show that the dynamical effects may vary strongly even in different configurations of the same model. To reduce this uncertainty a better understanding of tropical dynamics and model simulations without the necessity of gravity waver parameterizations, i.e.with horizontal resolutions at least an order of magnitude higher than used here, may be necessary. As for many questions related to CE, certainty of response would require the full implementation of CE. Observations of a prolonged westerly phase of the QBO (Labitzke, 1994) are weak due to the short lifetime of volcanic sulfate in the stratosphere.

Acknowledgements. We thank Simone Tilmes and Yaga Richter for inspiring discussions, Marco Giorgetta for valuable comments at different stages of the paper and Rene Hommel, Jan Kazil, Harri Kokkola and Hanna Vehkamäki for their earlier help to modify HAM. This work is a contribution to the German DFG-funded Priority Program 'Climate Engineering: Risks, Challenges, Opportunities?' (SPP 1689). U. Niemeier is supported by the SPP 1689 within the project CEIBRAL and CELARIT. Earlier parts of the study were funded by the German Environment Agency (UBA).

The simulations were performed on the computer of the Deutsches Klima Rechenzentrum (DKRZ). Information on model data used in this publication is available at http://www.mpimet.mpg.de/en/staff/ulrike-niemeier/geoengineering/data/

Atmos. Chem. Phys. Discuss., doi:10.5194/acp-2017-470, 2017
Manuscript under review for journal Atmos. Chem. Phys.
Discussion started: 29 May 2017

Atmospheric Chemistry and Physics
Discussions

References

Andrews, D. G., Holton, J. R., and Leovy, C. B.: Middle Atmosphere Dynamics, Academic Press, San Diego, CA, 1987.

Aquila, V., Garfinkel, C. I., Newman, P., Oman, L. D., and Waugh, D. W.: Modifications of the quasi-biennial oscillation by a geoengineering perturbation of the stratospheric aerosol layer, Geophys. Res. Lett., 41, 1738–1744, doi:10.1002/2013GL058818, 2014.

Baldwin, M. P., Gray, L. J., Dunkerton, T. J., Hamilton, K., Haynes, P. H., Randel, W. J., Holton, J. R., Alexander, M. J., Hirota, I., Horinouchi, T., Jones, D. B. A., Kinnersley, J. S., Marquardt, C., Sato, K., and Takahashi, M.: The quasi–biennial oscillation, Rev. Geophys., 39, 179–229, 2001.

Bittner, M., Schmidt, H., Timmreck, C., and Sienz, F.: Using a large ensemble of simulations to assess the Northern Hemisphere stratospheric dynamical response to tropical volcanic eruptions and its uncertainty, Geophysical Research Letters, 43, 9324–9332, doi:10.1002/2016GL070587, 2016GL070587, 2016.

Bowman, K.: Rossby wave phase speeds and mixing barriers in the stratosphere. Part I: Observations, J. Atmos. Sci., 52, 905–916, doi:10.1175/1520-0469(1996)053<0905:RWPSAM>2.0.CO;2, 1996.

Budyko, M. I.: Climatic changes, American Geophysical Society, Washington, D.C., doi:10.1029/SP010, 1977.

Butchart, N., A. S., Bourqui, M., de Garndpre, J., Hare, S., Kettleborough, J., Langematz, U., Manzini, E., Sassi, F., Shibata, K., Shindell, D., and Sigmond, M.: Simulations of anthropogenic change in the strength of the Brewer Dobson circulation, Clim. Dyn., 27, 727–741, doi:10.1007/s00382, 2006.

Butchart, N.: The Brewer-Dobson circulation, Rev. Geophys., 52, 157–184, doi:10.1002/2013RG000448, 2014.

Crutzen, P. J.: Albedo enhancement by stratospheric sulfur injections: A contribution to resolve a policy dilemma?, Clim Change, 77, 211–219, 2006.

English, J. M., Toon, O. B., and Mills, M. J.: Microphysical simulations of sulfur burdens from stratospheric sulfur geoengineering, Atmos. Chem. Phys., 12, 4775–4793, doi:10.5194/acp-12-4775-2012, 2012.

English, J. M., Toon, O., and M.J., M.: Microphysical simulations of large volcanic eruptions: Pinatubo and Toba, J. Geophys. Res. Atmos., 118, 1880–1895, doi:10.1002/jgrd.50196, 2013.

Giorgetta, M. A., Manzini, E., Roeckner, E., Esch, M., and Bengtsson, L.: Climatology and forcing of the quasi–biennial oscillation in the MAECHAM5 model, J. Climate, 19, 3882–3901, 2006.

Haynes, P. and Shuckburgh, E.: Effective diffusivity as a diagnostic of atmospheric transport. I- Stratosphere, Journal of geophysical research, 105, 22, 2000.

Haywood, J., Jones, A., Bellouin, N., and Stephenson, D.: Asymmetric forcing from stratospheric aerosols impacts Sahelian rainfall, Nature Climate Change, 3, 660–665, doi:10.1038/nclimate1857, 2013.

Holton, J. R., Haynes, P. H., McIntyre, M. E., Douglass, A. R., Rood, R. R., and Pfister, L.: Stratospheric–tropospheric exchange, Rev. Geophys., 33, 403–439, 1995.

Hommel, R., Timmreck, C., and Graf, H. F.: The global middle-atmosphere aerosol model MAECHAM5-SAM2: comparison with satellite and in-situ observations, Geoscientific Model Development, 4, 809–834, doi:10.5194/gmd-4-809-2011, http://www.geosci-model-dev.net/4/809/2011/, 2011.

Kravitz, B., Caldeira, K., Boucher, O., Robock, A., Alterskjær, P. J. R. K., Karam, D. B., Cole, J. N. S., Curry, C. L., Haywood, J. M., Irvine, P. J., Ji, D., Jones, A., Kristjánsson, J. E., Lunt, D. J., Moore, J. C., Niemeier, U., Schmidt, H., Schulz, M., Singh, B., Tilmes, S., Watanabe, S., Yang, S., and Yoon, J.-H.: Climate model response from the Geoengineering Model Intercomparison Project (GeoMIP), J. Geophys. Res., 118, 8320–8332, doi:10.1002/jgrd.50646, 2013.

Laakso, A., Korhonen, H., Romakkaniemi, S., and Kokkola, H.: Radiative and climate effects of stratospheric sulfur geoengineering using seasonally varying injection areas, Atmospheric Chemistry and Physics Discussions, 2017, 1–25, doi:10.5194/acp-2017-107, http://www.atmos-chem-phys-discuss.net/acp-2017-107/, 2017.

Labitzke, K.: Stratospheric temperature changes after the Pinatubo eruption, Journal of Atmospheric and Terrestrial Physics, 56, 1027–1034, doi:10.1016/0021-9169(94)90039-6, http://www.sciencedirect.com/science/article/pii/0021916994900396, middle Atmosphere Science, 1994.

Moriyama, R., Sugiyama, M., Kurosawa, A., Masuda, K., Tsuzuki, K., and Ishimoto, Y.: The cost of stratospheric climate engineering revisited, Mitigation and Adaptation Strategies for Global Change, pp. 1–22, doi:10.1007/s11027-016-9723-y, http://dx.doi.org/10.1007/s11027-016-9723-y, 2016.

Niemeier, U. and Timmreck, C.: What is the limit of climate engineering by stratospheric injection of SO2?, Atmospheric Chemistry and Physics, 15, 9129–9141, doi:10.5194/acp-15-9129-2015, http://www.atmos-chem-phys.net/15/9129/2015/, 2015.

Niemeier, U., Timmreck, C., Graf, H.-F., Kinne, S., Rast, S., and Self, S.: Initial fate of fine ash and sulfur from large volcanic eruptions, Atmospheric Chemistry and Physics, 9, 9043–9057, http://www.atmos-chem-phys.net/9/9043/2009/, 2009.

Niemeier, U., Schmidt, H., and Timmreck, C.: The dependency of geoengineered sulfate aerosol on the emission strategy, Atmos. Sci. Let., 12, 189–194, doi:10.1002/asl.304, 2011.

Niemeier, U., Schmidt, H., Alterskjær, K., and Kristjánsson, J. E.: Solar irradiance reduction via climate engineering – Impact of different techniques on the energy balance and the hydrological cycle, JGR, 118, 11 905–11 917, doi:10.1002/2013JD020445, 2013.

O'Sullivan, D. and Chen, P.: Modeling the quasi biennial oscillation's influence on isentropic tracer transport in the subtropics, J. Geophys. Res., 101, 6811–6821, 1996.

Pierce, J. R., Weisenstein, D. K., Heckendorn, P., Peter, T., and Keith, D. W.: Efficient formation of stratospheric aerosol for climate engineering by emission of condensible vapor from aircraft, GRL, 37, L18 805, doi:10.1029/2010GL043975, 2010.

Plumb, R. A.: A tropical pipe model of stratospheric transport, J. Geophys. Res., 101, 3957–3972, 1996.

Plumb, R. A. and Bell, R. C.: A model of quasibiennial oscillation on an equatorial beta–plane, Q. J. R. Meteorol. Soc., 108, 335–352, 1982.

Punge, H. J., Konopka, P., Giorgetta, M. A., and Müller, R.: Effects of the quasi-biennial oscillation on low-latitude transport in the stratosphere derived from trajectory calculations, J. Geophys. Res., 114, D03 102, doi:10.1029/2008JD010518, 2009.

Robock, A.: Volcanic eruptions and climate, Rev. Geophys., 38, 191–219, 2000.

Roeckner, E., Baeuml, G., Bonaventura, L., Brokopf, R., Esch, M., Giorgetta, M., Hagemann, S., Kirchner, I., Kornblueh, L., Manzini, E., Rhodin, A., Schlese, U., Schulzweida, U., and Tompkins, A.: The atmospheric gernal circulation model ECHAM5 - Part I, MPI Report No. 349, p. 127, 2003.

Schmidt, H., Alterskjær, K., Bou Karam, D., Boucher, O., Jones, A., Kristjánsson, J. E., Niemeier, U., Schulz, M., Aaheim, A., Benduhn, F., Lawrence, M., and Timmreck, C.: Solar irradiance reduction to counteract radiative forcing from a quadrupling of CO_2: climate responses simulated by four earth system models, Earth System Dynamics, 3, 63–78, doi:10.5194/esd-3-63-2012, 2012.

Shindell, D., Schmidt, G., Mann, M., , and Faluvegi, G.: Dynamic winter climate response to large tropical volcanic eruptions since 1600, J. Geophys. Res., 21, 2587–2590, doi:10.1029/2003JD004151, 2004.

Shuckburgh, E., Norton, W., Iwi, A., and Haynes, P.: Influence of the quasi–biennial oscillation on isentropic transport and mixing in the tropics and subtropics, J. Geophys. Res., 106, 14 327–14 337, 2001.

Stier, P., Feichter, J., Kinne, S., Kloster, S., Vignati, E., Wilson, J., Ganzeveld, L., Tegen, I., Werner, M., Balkanski, Y., Schulz, M., Boucher, O., Minikin, A., and Petzold, A.: The aerosol–climate model ECHAM5–HAM, Atmos. Chem. Phys., 5, 1125–1156, 2005.

Tilmes, S., Müller, R., and Salawitch, R.: The sensitivity of polar ozone depletion to proposed geoengineering schemes, Science, 320(5880), 1201–1204, doi:10.1126/science.1153966, 2008.

Tilmes, S., Fasullo, J., Lamarque, J.-F., Marsh, D., Mills, M., Alterskjær, K., Boucher, O., Cole, J., Curry, C., Haywood, J., Irvine, P., Ji, D., Jones, A., BouKaram, D., Kravitz, B., Kristjánsson, J. E., Moore, J., Muri, H. O., Niemeier, U., Rasch, P. J., Robock, A., Schmidt, H., Schulz, M., Shuting, Y., B.Singh, Watanabe, S., and Yoon, J.-H.: The Hydrologic Impact of Geoengineering in the Geoengineering Model Intercomparison Project (GeoMIP), under review for J. Geophys. Res., 118 (19), 11 036–11 058, doi:10.1002/jgrd.50868, 2013.

Timmreck, C.: Three–dimensional simulation of stratospheric background aerosol: First results of a multiannual general circulation model simulation, J. Geophys. Res., 106, 28 313–28 332, 2001.

Timmreck, C., Graf, H.-F., and Kirchner, I.: A one and half year interactive MA/ECHAM4 simulation of Mount Pinatubo Aerosol, J. Geophys. Res., 104, 9337–9360, doi:10.1029/1999JD900088, 1999.

Toohey, M., Krüger, K., Niemeier, U., and Timmreck, C.: The influence of eruption season on the global aerosol evolution and radiative impact of tropical volcanic eruptions, ACP, 11, 12 351–12 367, doi:10.5194/acp-11-12351-2011, 2011.

Trepte, C. R. and Hitchman, M. H.: Tropical stratospheric circulation deduced from satellite aerosol data, Nature, 355, 626–628, 1992.